This article has been accepted for publication in a future issue of this journal, but has not been fully edited. Content may change prior to final publication. Citation information: DOI 10.1109/TSG.2021.3063960, IEEE Transactions on Smart Grid

Peer-to-Peer Energy Trading in Transactive Markets Considering Physical Network Constraints

Md Habib Ullah, *Student Member, IEEE,* Jae-Do Park, *Senior Member, IEEE*

***Abstract*—In recent years, the rapid growth of active consumers in the distribution networks transforms the modern power markets' structure more independent, flexible, and distributed. Specifically, in the recent trend of peer-to-peer (P2P) transactive energy systems, the traditional consumers became prosumers (producer+consumer) who can maximize their energy utilization by sharing it with neighbors without any conventional arbitrator in the transactions. Although a distributed energy pricing scheme is inevitable in such systems to make optimal decisions, it is challenging to establish under the influence of non-linear physical network constraints with limited information. Therefore, this paper presents a distributed pricing strategy for P2P transactive energy systems considering voltage and line congestion management, which can be utilized in various power network topologies. This paper also introduces a new mutual reputation index as a product differentiation between the prosumers to consider their bilateral trading willingness. In this paper, a Fast Alternating Direction Method of Multipliers (F-ADMM) algorithm is realized instead of the standard ADMM algorithm to improve the convergence rate. The effectiveness of the proposed approach is validated through software simulations. The result shows that the algorithm is scalable, converges faster, facilitates easy implementation, and ensures maximum social welfare/profit.**

***Index Terms*—Distributed optimization, Energy pricing, Peer-to-peer market, Transactive energy, and Smart grid.**

NOMENCLATURE

Abbreviations

ADMM	Alternating direction method of multipliers
MRI	Mutual reputation index
NUF	Network utilization fee
P2P	Peer-to-peer
PUSC	Per unit service charge
TE	Transactive energy

Indices and sets

$\mathcal{C}$	Set of consumers
$\mathcal{L}$	Set of line segments, $l \in \mathcal{L}$
$\mathcal{N_B}$	Set of busses in the distribution network
$\mathcal{N}$	Set of prosumers, $i, j \in \mathcal{N}$
$\mathcal{N}_i$	Set of trading neighbors of prosumer i
$\mathcal{P}$	Set of producers
$\mathcal{T}$	Set of time steps, $t \in \mathcal{T}$
Υ_j	Set of bus j's downstream neighbouring buses

Parameters

α_i, β_i	Cost function parameters of prosumer i
η	Small penalty factor
γ	Unit service charge for NUF
$\lambda_{i,j}$	Network utilization fee between traders i and j
$\overline{\mathbf{W}}$	Graph incidence matrix of distribution network
$\mathbf{R}, \mathbf{X}$	Network resistance and reactance matrices
$\omega_{i,j}$	Reputation function between traders i and j
$\sigma_{i,j}$	Mutual reputation index between traders i and j
φ	Scaling factor for mutual reputation index
ξ	Small tuning parameter
c	Reputation benefit for per unit energy transaction between traders i and j
$d_{i,j}$	Net electrical distance between traders i and j
$f_l^{\min}, f_l^{\max}$	Minimum and maximum power flows at line l
k	Iteration index
N	Total number of prosumers
$p_i^{\min}, p_i^{\max}$	Minimum and maximum power limits of prosumer i
$r_{i,j}, x_{i,j}$	Resistance and reactance of line segment between buses i and j
t	Time index
$v_i^{\min}, v_i^{\max}$	Minimum and maximum voltage at prosumer's bus i

Variables

$\boldsymbol{\rho}$	Auxiliary variable for coupling constraints
$\boldsymbol{\tau}, \boldsymbol{\phi}$	Lagrangian variables
$\mathbf{P}, \mathbf{Q}$	Vectors of real and reactive power flows
$\mathbf{p}, \mathbf{v}$	Bus injected power and voltage vectors
μ_i	Acceleration operator for prosumer i
$\pi_{i,j}/\pi_{j,i}$	Dual variable and price signal between energy prosumers i and j
f_l	Real power flow in line l
p_i	Power set point of prosumer at bus i
$P_{i,j}, Q_{i,j}$	Real and reactive power flows from bus i to j
$p_{i,j}/p_{j,i}$	Traded power between prosumers i and j
v_i	Voltage at prosumer's bus i

Manuscript received June 30, 2020; revised October 12, 2020, December 09, 2020; accepted February 24, 2021. This work was supported by the National Science Foundation grant ECCS-1554626.

M.H. Ullah and J.D. Park are with the Electrical Engineering Department, University of Colorado Denver, 1200 Larimer Street, Denver, Colorado 80217-3364, USA. (e-mail: md.ullah@ucdenver.edu; jaedo.park@ucdenver.edu).

Corresponding author is Dr. Jae-Do Park; jaedo.park@ucdenver.edu.

I. INTRODUCTION

A. Background

IN modern power systems, the integration of distributed energy resources, such as renewable energy sources, energy storage systems, electric vehicles, flexible loads, and so on, has substantially increased. For instance, it is expected that the global market for rooftop photovoltaic (PV) panels will be worth about $33 billion by 2022, and the increase in adoption of residential energy storage systems complements the shift towards distributed generation even further, whose capacity is predicted to grow more than 3.7 GW by 2025 [1]. These additional energy resources at the edge of the grid are needed to be utilized more efficiently not only to manage the

This article has been accepted for publication in a future issue of this journal, but has not been fully edited. Content may change prior to final publication. Citation information: DOI 10.1109/TSG.2021.3063960, IEEE Transactions on Smart Grid

energy demand but also to enable a significant penetration of renewable energy into the grid.

In the given context, transactive energy (TE) concept has emerged for the future smart grid operations, which is a market-based approach to systematically coordinate the energy generation and consumption among the entities across the network. It opens new opportunities for existing stakeholders, including retailers, policymakers, residential, industrial, and commercial users with well-designed economic incentives [2], [3]. Concurrently, TE systems create significant challenges in smart grid operation regarding optimum power flows, stability and reliability of the grids, energy market efficiencies, and others [4], [5]. Along with network management and control features, the TE frameworks provide competitive electricity market environments, namely transactive markets, for the energy producers and consumers via two-way information exchange with standardized protocols.

In TE systems, the conventional passive consumers become active prosumers (producer+consumer) with generating assets, such as roof top PV panels. The role of prosumers is well recognized in the TE markets. The two dominant schemes for compensating the prosumers for the energy they feed back into the grid are net-metering and feed-in tariff (FiT) programs [1]. However, the high penetration of PVs in the grids raised stability and reliability issues; hence, the local governments in many countries are now limiting the PV energy export to the grid [6]. Moreover, the prosumers are getting paid at a fixed rate in both the schemes [1]. Typically, prosumers lose potential benefits by buying energy from the grid at a high price and getting paid low prices when they sell.

As a solution, peer-to-peer (P2P) energy sharing concept has gained attention as a prominent alternative solution in the TE frameworks [2], [4], [7]. Unlike the traditional systems, the P2P scheme enables the prosumers to participate in local energy trading with the neighboring prosumers. The P2P distributed market platforms are currently possible due to continuing advances in information and communication technology, multi-agent systems, and distributed ledger technologies such as blockchain, which support transparent and decentralized transactions. However, efficient energy pricing in such TE systems is an important task to accomplish. Concurrently, the physical network constraints need to be considered in the pricing model to implement real-time TE systems.

B. Related Research

In recent literature, various approaches have been presented for P2P energy trading in distribution systems. For instance, an auction-based P2P energy trading model is introduced for prosumer-centric community microgrids [8]. In [9], a P2P energy trading paradigm has been presented with various pricing strategies such as bill sharing, mid-market rate, and auction-based schemes, and various scenarios were compared. In addition to the mid-market rate, a canonical coalition game-theoretic model has been adopted for prosumer-centric microgrids in [6]. A two-stage bidding strategy for P2P energy trading is proposed in residential microgrids in [10]. In [11], a P2P energy sharing model for distribution systems is described. However, these approaches require a central coordinator in transactions, which makes the privacy of the prosumers' as an utmost concern besides the scalability issues.

Afterward, various distributed trading approaches have been developed, wherein no intermediary interference is required. For example, bilateral energy trading strategies using relaxed consensus+innovation algorithm have been designed in [12], [13]. These approaches considered product differentiation through implementation of network tariffs, which reflects the prosumers' preference on type and quantity of the energy they may exchange. In addition, prosumers' preference-driven P2P multi-class energy trading model is presented using alternating direction method of multipliers (ADMM) [14]. Ref. [15] presents a dynamic energy pricing strategy for P2P TE systems in smart grid. In [16], an incentive model for distributed energy trading is presented for a power-heat-gas combined system using an ADMM optimization approach. In [17]–[19], ADMM and game-theoretic two-stage energy sharing models have been studied for prosumer-centric smart buildings and microgrids. In such approaches, prosumers determine the amount of shared energy in the first stage and negotiate the price in the second stage. Social welfare maximization based on dual-decomposition and Stackelberg game is proposed for P2P energy trading in [20], [21]. Ref. [22] describes a game-theoretic P2P energy sharing model for multi-regional distribution networks. A blockchain-based localized P2P electricity trading model is proposed for plug-in hybrid electric vehicle systems in [23]. Supported by simulation results, the researches in [12]–[23] explain bilateral trading mechanism in P2P transactive market well. However, the network constraints such as bus voltage and line power flow limits have been largely neglected in energy trading, which is impractical in actual power distribution networks.

In the given context, line power flow constraints have been addressed in P2P energy transactions using power transfer distribution factors (PTDFs) in [24], but it requires a central coordinator and does not allow bilateral energy trading with negotiated prices between multiple producers and consumers. A PTDF-based energy sharing model is proposed enabling multiple bilateral trading between prosumers in [25]; although line capacity constraints were considered using approximated DC power flow method, bus voltage constraints were excluded. It is important to note that, due to the high resistance to reactance ratio in the connected lines, the bus voltages are highly susceptible to any deviation of active power injection in the distribution networks [26]. In [27], a decentralized P2P energy sharing methodology has been demonstrated for a low-voltage network that considers the distribution network constraints before each transaction through voltage sensitivity coefficients, PTDFs, and loss sensitivity factors. However, the total social welfare of the system hasn't been considered in this approach. In [28], an iterative co-optimization strategy for prosumers' social welfare maximzation that couples P2P trasactions and distribution network management has been presented. This approach meets the network constraints imposing network utilization fees but it may lead to a sub-optimal solution in various scenarios. Ref. [29] proposed a new approach that reduces the violations of distribution network constraints. This technique integrates P2P energy trading with the local energy trading using day-ahead unidirectional pricing signals. Although the approaches in [27] and [29] may be effective for small amount of energy exchange, it could result in voltage limit violations with significant number of distributed energy resources in the distribution networks. Moreover, [27]–[29] did not consider the direct impact of the physical network constraints in the P2P energy pricing. It is important to note that the bilateral pricing in P2P trading plays a significant role in determining the prosumers' power set points; hence, any change in price will apparently affect the bus voltages and line power flows and vice-versa. Another important aspect that have not been extensively studied is the market participants' willingness in energy trading with a specific or a group of energy traders. Typically, bilateral trades may highly be influenced by the traders' previous transaction experiences.

Motivated by these discussions, this paper intends to develop a network-constrained distributed bilateral energy pricing scheme that maximizes total welfare of the system in the P2P transactive markets; it also ensures prosumers' privacy and considers direct influence of network constraints in the bilateral energy pricing. The presented approach should prevent any violation of the line power flow and the bus voltage limits in physical networks regardless of the amount of the energy transactions. Moreover, the trading willingness of the market participants needs to be quantified based on bilateral relationship in order to include it in the P2P energy pricing.

C. Major Contributions

The major contributions of this paper can be summarized as follows:

- A bilateral energy trading scheme with a novel reputation-based product differentiation model is presented for coordinated interactions between prosumers in the P2P transactive energy market. The network utilization fee is considered as well.
- A distributed energy pricing algorithm for the market participants is proposed using an F-ADMM-based optimization technique and a closed-form solution was derived to reduce the computational time.
- Physical network constraints are explicitly integrated in the energy pricing in terms of line-congestion and bus voltage management, and the effect is briefly analyzed. These were modeled using the simplified LinDistFlow method for distribution networks in tree-topology. Design methodology for mesh networks is also demonstrated in the Appendix.
- The proposed approach is scalable, allows more prosumers to participate in the P2P energy trading, and it converges faster compared to the existing algorithms.

D. Paper Organization

The rest of this paper is organized as follows: Section II demonstrates the power distribution system modeling, Section III describes mathematical modeling of the prosumers' cost functions and the centralized optimization problem formulation for bilateral energy trading. The proposed distributed P2P energy trading scheme with closed-form solution is presented in Section IV. Section V shows the simulation result and analysis followed by Section VI that concludes the paper.

II. Power Distribution System Modelling

Consider a tree-topology radial power distribution network denoted by a set of buses $\mathcal{N}_{\mathcal{B}} := \{0, 1, ..., N\}$ and a set of line segments $\mathcal{L} := \{l \to (i,j)\} \subseteq \mathcal{N}_{\mathcal{B}} \times \mathcal{N}_{\mathcal{B}}$. In a tree-topology distribution network, the number of line segments $|\mathcal{L}| = (N+1) - 1 = N$. The bus 0 assumed to be the reference bus with 1 per unit (p.u.) voltage. For every bus i, let v_i denote its voltage magnitude, p_i and q_i represent the active and reactive power injections, respectively. Let $r_{i,j}$ and $x_{i,j}$ symbolize resistance and reactance of line segment (i, j), and $P_{i,j}$ and $Q_{i,j}$ are the real and reactive power flow through this line. Define $\Upsilon_j \subset \mathcal{N}$ is the bus j's downstream neighbouring buses. For a given line $l \to (i,j) \in \mathcal{L}$, the network branch flow can be described using the DistFlow model [30], [31]:

$$P_{i,j} = -p_j + \sum_{m\in\Upsilon_j} P_{j,m} + r_{i,j} l_{i,j}, \tag{1a}$$

$$Q_{i,j} = -q_j + \sum_{m\in\Upsilon_j} Q_{j,m} + x_{i,j} l_{i,j}, \tag{1b}$$

$$v_j^2 = v_i^2 - 2\big(r_{i,j}P_{i,j} + x_{i,j}Q_{i,j}\big) + \big(r_{i,j}^2 + x_{i,j}^2\big) l_{i,j}, \tag{1c}$$

$$l_{i,j} = \frac{P_{i,j}^2 + Q_{i,j}^2}{v_i^2}. \tag{1d}$$

In (1), the quadratic term $l_{i,j}$ makes the problem non-convex. To make it convex, the real and reactive power loss $r_{i,j}l_{i,j}$ and $x_{i,j}l_{i,j}$, as well as $r_{i,j}^2 l_{i,j}$ and $x_{i,j}^2 l_{i,j}$, are neglected considering that the losses are much smaller than the power flow $P_{i,j}$ and $Q_{i,j}$, which is typically on the order of 1% [31]. Hence, applying a flat voltage profile approximation, i.e., $v_i \approx 1,\ \forall i \in \mathcal{N}_{\mathcal{B}}$, it can be obtained that $v_j^2 - v_i^2 \approx 2(v_j - v_i)$. Adopting this assumption in (1c), the linearized DistFlow (LinDistFlow) model can be given as [32]:

$$P_{i,j} - \sum_{m\in\Upsilon_j} P_{j,m} = -p_j, \tag{2a}$$

$$Q_{i,j} - \sum_{m\in\Upsilon_j} Q_{j,m} = -q_j, \tag{2b}$$

$$v_i - v_j = r_{i,j}P_{i,j} + x_{i,j}Q_{i,j}. \tag{2c}$$

At this instant, (2) can be summarized in a matrix form as:

$$-\mathbf{W}^T\mathbf{P} = -\mathbf{p}, \tag{3a}$$

$$-\mathbf{W}^T\mathbf{Q} = -\mathbf{q}, \tag{3b}$$

$$\overline{\mathbf{w}} + \mathbf{W}\mathbf{v} = \mathbf{F_r}\mathbf{P} + \mathbf{F_x}\mathbf{Q}, \tag{3c}$$

where $\mathbf{p}$ and $\mathbf{q}$ are the column matrices of bus injected real and reactive powers. Diagonal matrices $\mathbf{F_r}$ and $\mathbf{F_x}$ are $N \times N$ matrices whose l-th diagonal entries are composed by $r_{i,j}$ and $x_{i,j}$. Column matrix $\overline{\mathbf{w}}$ and matrix $\mathbf{W}$ of size $N \times N$ are the sub-matrices of graph incidence matrix $\overline{\mathbf{W}}$ of size $N \times (N+1)$, i.e., $\overline{\mathbf{W}} = [\overline{\mathbf{w}}\ \mathbf{W}]$. The entries of the graph incidence matrix are defined as $\overline{\mathbf{W}}_{l,i} = 1$ if a line l leaves bus i and $\overline{\mathbf{W}}_{l,i} = -1$ if line l enters bus i. Solving for $\mathbf{P}$ and $\mathbf{Q}$ and substituting them into (3c) yields,

$$\mathbf{v} = v_0\mathbf{1} + \mathbf{R}\mathbf{p} + \mathbf{X}\mathbf{q}, \tag{4}$$

where $\mathbf{1}$ is a column matrix with all elements of 1, and v_o is the predefined slack bus voltage, and $\mathbf{R} := \mathbf{W}^{-1}\mathbf{F_r}\mathbf{W}^{-T}$

This article has been accepted for publication in a future issue of this journal, but has not been fully edited. Content may change prior to final publication. Citation information: DOI 10.1109/TSG.2021.3063960, IEEE Transactions on Smart Grid

and $\mathbf{X} := \mathbf{W}^{-1}\mathbf{F_x}\mathbf{W}^{-T}$ can be viewed as network resistance and reactance matrices, respectively. The matrix $\mathbf{v}$ contains all the nodal voltages except the slack bus voltage. Viewing the injected reactive power $\mathbf{q}$ as a constant, the bus voltage vector in (4) can be written in terms of variable real power $\mathbf{p}$ as:

$$\mathbf{v} = \mathbf{R}\mathbf{p} + \bar{\mathbf{v}}, \tag{5}$$

where the fraction of voltage vector $\bar{\mathbf{v}} := v_0\mathbf{1} + \mathbf{X}\mathbf{q}$ is a constant term as $\mathbf{q}$ is considered to be constant in this paper and $\mathbf{v} = [v_1\ v_2\ ...\ v_i\ ...\ v_N]^T$. The real power flow in the lines, relating to $\mathbf{p}$, can be given from (3a) as:

$$\mathbf{P} = \mathbf{W}^{-T}\mathbf{p} = \mathbf{A}\mathbf{p}, \tag{6}$$

where $\mathbf{A} := \mathbf{W}^{-T}$. Let $\mathbf{P} = [f_1\ f_2\ ...f_l\ ...\ f_N]^T$, where f_l is the power flow in line l, which is equivalent to $P_{i,j}$. However, it can be noticed from (5) and (6) that the bus voltages and line power flows can be expressed with regard to the injected bus power $\mathbf{p}$ through $\mathbf{R}$ and $\mathbf{A}$. These attributes will be utilized in the Section IV to solve the bilateral energy trading problem.

Remark 1 *We utilized the linear LinDistFlow model for power flow analysis over the convex second-order conic DistFlow [30] approach. Although the exactness of the solution may be slightly compromised with the LinDistFlow model, it is advantageous for low computational complexity and higher efficiency. However, further research can be conducted for trade-off between the solution exactness, computational efficiency, and reliability, which is beyond the scope of this paper.*

III. Preliminaries and Problem Formulation

Consider a smart distribution network comprises of a set of prosumers $\mathcal{N} := \{1, 2, ..., N\}$ with index $i \in \mathcal{N}$, where $N = |\mathcal{N}|$ is the cardinality, which gives the total number of prosumers in the system. Suppose there $\mathcal{P} := \{\mathcal{P}_a : \forall a \in \mathcal{N}\}$ is the set of producers and $\mathcal{C} := \{\mathcal{C}_b : \forall b \in \mathcal{N}\}$ is the set of consumers. It should be noted that $\mathcal{N} = \mathcal{P} \cup \mathcal{C}$ and $\mathcal{P} \cap \mathcal{C} = \emptyset$. Both the $\mathcal{P}$ and $\mathcal{C}$ are connected in the physical power distribution network. Let $\mathcal{T} := \{1, 2, ..., T\}$ is a set of time steps with index $t \in \mathcal{T}$. In this paper, only producer-to-consumer connections are required and no energy storage system was considered.

A. Role of a Prosumer

In this paper, it is assumed that the prosumers are located in residential areas with rooftop PV panels which are connected to the network through a smart meter. The household loads that the prosumers own are classified into controllable and uncontrollable loads. In each time step, the prosumers declare themselves as a producer or a consumer based on their net load, which can be determined as:

$$p_{i,t} = p^g_{i,t} - (p^{lc}_{i,t} + p^{ln}_{i,t}), \quad \forall i \in \mathcal{N}, \quad \forall t \in \mathcal{T}, \tag{7}$$

where $p^g_{i,t}$ is the amount of power generation from rooftop solar panels, $p^{lc}_{i,t}$ and $p^{ln}_{i,t}$ are the amounts of controllable and uncontrollable loads. If $p^g_{i,t} > (p^{lc}_{i,t} + p^{ln}_{i,t})$ then market participant i is a producer and $p^g_{i,t} < (p^{lc}_{i,t} + p^{lc}_{i,t})$ if i is a consumer. It should be noted that no flexible loads with time-coupling constraints are considered in this paper. Our main objective is to integrate the impact of network constraints in the energy pricing with product differentiation. Thus, the flexible load is disregarded in this work, although it can be included in this system with proper mathematical modelling.

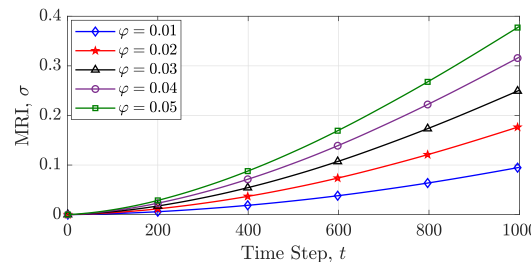

Fig. 1: Mutual reputation index (MRI) for various scaling factor φ.

B. Reputation-based Product Differentiation

Typically, bilateral trades are highly influenced by the traders' previous relation and experience. Prosumers may prefer to negotiate with trading partners of higher reputation value determined based on their past performance in successful energy transactions. Hence, we define a mutual reputation index (MRI) between the traders that can be quantified in a distributed way at each end. At a time step t, the MRI between producer i and consumer j can be calculated as:

$$\sigma_{i,j,t} = \sigma_{i,j,t-1} + \varphi \frac{\pi_{i,j,t-1}|p_{i,j,t-1}|}{\sum_{y=1}^{Y} \pi_{i,j,y}|p_{i,j,y}|}, \tag{8}$$

where φ is a small positive scaling factor (impact of φ on MRI is shown in Fig. 1), Y is the total number of transactions from the initial participation to till the time step $t-1$, and $\sigma_{i,j,t-1}$ is the MRI at the previous time step. In the second term of the right hand side of (8), the numerator represents the payment in last transaction and the denominator gives total payment up to the previous time steps. It signifies that each transaction adds a non-negative value to the MRI regardless of energy price ($\pi_{i,j}$) and amount ($p_{i,j}$), and a higher payment leads to a higher MRI. The initial MRI between two market participants should be set to 0 and it remains 0 until a successful energy trading happens. It should be noted that $\sigma_{i,j} = \sigma_{j,i}$ at any point of market operation. Now, the bilateral trading reputation function can be quantified as:

$$\omega_{i,j,t} = \hat{c}\sigma_{i,j,t}, \tag{9}$$

where $\hat{c} = \varrho c$ and c is the reputation benefit for per unit energy transaction. The parameter ϱ is unity and it is positive and negative for producers and consumers, respectively.

C. Network Utilization Fees

There will be a service charge for using power network infrastructure that the market participants need to pay for each trade. The network owners may set a network utilization fee (NUF) prior to P2P market clearings, considering network maintenance cost, grid modernization charge, taxes and policies etc. [13]. Inspired from [33], we design a new NUF in this paper based on the net electrical distance, which can be written as:

$$\lambda_{i,j} = \hat{\gamma} d_{i,j}, \tag{10}$$

This article has been accepted for publication in a future issue of this journal, but has not been fully edited. Content may change prior to final publication. Citation information: DOI 10.1109/TSG.2021.3063960, IEEE Transactions on Smart Grid

where $\hat{\gamma} = \varrho\gamma$ and γ represents the per unit service charge (PUSC) for an unit of energy to transport in each unit of electrical distance. The unity parameter ϱ is positive for producers and negative for consumers. The parameter $d_{i,j}$ is the electrical distance between market participants i and j that takes into account the aggregated impedances of the connected branches between bus i and j as:

$$d_{i,j} = \sum_{l \in \mathcal{L}_{i,j}} |z_l|, \tag{11}$$

where z_l is the impedance of line l and $\mathcal{L}_{i,j}$ collects the lines between buses i and j. It is straightforward to compute $d_{i,j}$ for tree-type distribution networks. For example in Fig. 2, the net electrical distance between buses 9 and 7 is $d_{97} = |z_{9,8}| + |z_{8,1}| + |z_{1,5}| + |z_{5,7}|$. In mesh networks with multiple routes between i and j, shortest path algorithms can be considered [34]. However, the payment with NUF is paid to the network owner and the network manager who maintains the system without violating the bus voltage and line power flow constraints.

D. Bilateral Trading Problem Formulation

Let $\hat{p}_{i,t} = \{p_{i,j,t}, \forall j \in \mathcal{N}_i, \forall t \in \mathcal{T}\}$ be a set of the traded power between prosumer i and its neighbors $\forall j \in \mathcal{N}_i$, where $\mathcal{N}_i$ is the set of neighbours with whom prosumer $i, \forall i \in \mathcal{N}$, trades in the TE market. To avoid energy sharing between producer-to-producer or consumer-to-consumer, it should be considered that if i is a producer then j is a consumer, and vice-versa. The traded power $p_{i,j,t}$ at time step t is positive and negative when the prosumer i sells and buys power to/from j, respectively. Therefore, $p_{i,j,t}$ and $p_{j,i,t}$ are equal valued but in opposite polarity and each prosumer $i \in \mathcal{N}, j \in \mathcal{N}_i$ should satisfy the following reciprocity coupled constraint:

$$p_{i,j,t} + p_{j,i,t} = 0, \quad \forall t \in \mathcal{T}. \tag{12}$$

The cost/utility function of prosumers typically quantifies their satisfaction level on sharing a certain amount of power. Logarithmic and quadratic utility functions have been frequently used for modeling the utility functions. Without losing generality, a quadratic cost function for producers and utility function for consumers is considered in this paper as [23]:

$$u_i(\hat{p}_{i,t}) = \alpha_i \sum_{j \in \mathcal{N}_i} p_{i,j,t}^2 + \beta_i \sum_{j \in \mathcal{N}_i} p_{i,j,t}, \quad \forall t \in \mathcal{T}, \tag{13}$$

where $\alpha_i > 0$ and $\beta_i \geq 0$ are the cost function coefficients from prosumer i. The power $p_{i,j,t}$ is positive and negative for the producers and consumers, respectively. The cost function associated with the network utilization fees can be written as:

$$n_i(\hat{p}_{i,t}) = \sum_{j \in \mathcal{N}_i} \lambda_{i,j,t} p_{i,j,t}, \quad \forall t \in \mathcal{T}, \tag{14}$$

and the reputation cost function can be given as:

$$r_i(\hat{p}_{i,t}) = \sum_{j \in \mathcal{N}_i} \omega_{i,j,t} p_{i,j,t}, \quad \forall t \in \mathcal{T}. \tag{15}$$

From the social perspective, the localized P2P electricity trading should maximize social welfare by maximizing energy traders' reputation and by minimizing their cost functions while achieving a market equilibrium. Therefore, the total social welfare of the system can be expressed as:

$$\mathcal{S}_{\mathcal{W}} = \sum_{t \in \mathcal{T}} \sum_{i \in \mathcal{N}} \big[r_i(\hat{p}_{i,t}) - u_i(\hat{p}_{i,t}) - n_i(\hat{p}_{i,t}) \big]. \tag{16}$$

In the P2P trading scheme, the power set point $p_{i,t}$ of each prosumer at time step t can be given as the sum of all the P2P traded quantities as:

$$p_{i,t} = \sum_{j \in \mathcal{N}_i} p_{i,j,t}, \quad \forall t \in \mathcal{T}. \tag{17}$$

Let the producer $i \in \mathcal{P}$ and consumer $j \in \mathcal{C}$ privately negotiate the price for the traded power $p_{i,j}$ as $\pi_{i,j}$. The following condition should be satisfied considering the balance of payments in each pair of producer and consumer as:

$$\pi_{i,j,t} = \pi_{j,i,t}, \quad \forall t \in \mathcal{T}. \tag{18}$$

It should be noted that $p_{i,j,t}$ and $\pi_{i,j,t}$ are the traded power and unit price determined by i at time t; and similarly, $p_{j,i,t}$ and $\pi_{j,i,t}$ are the traded power and price determined by j at time t.

The bilateral energy trading problem can be formulated to maximize the combined social welfare or to minimize the overall cost of the prosumers. Therefore, the centralized optimization problem $\forall t \in \mathcal{T}$ is designed as:

$$\min_{p_{i,j}} \quad \sum_{t \in \mathcal{T}} \sum_{i \in \mathcal{N}} u_i(\hat{p}_{i,t}) + n_i(\hat{p}_{i,t}) - r_i(\hat{p}_{i,t}), \tag{19a}$$

$$\text{s.t.} \quad p_{i,t}^{\min} \leq p_{i,t} \leq p_{i,t}^{\max}, \qquad \forall i \in \mathcal{N}, \tag{19b}$$

$$v_{i,t}^{\min} \leq v_{i,t} \leq v_{i,t}^{\max}, \qquad \forall i \in \mathcal{N}_{\mathcal{B}} \backslash \{0\}, \tag{19c}$$

$$f_{l,t}^{\min} \leq f_{l,t} \leq f_{l,t}^{\max}, \qquad \forall l \in \mathcal{L}, \tag{19d}$$

$$p_{i,j,t} + p_{j,i,t} = 0, \qquad \forall i \in \mathcal{N}, \quad \forall j \in \mathcal{N}_i, \tag{19e}$$

$$p_{i,j,t} \geq 0, \qquad \forall i \in \mathcal{P}, \quad \forall j \in \mathcal{N}_i, \tag{19f}$$

$$p_{i,j,t} \leq 0, \qquad \forall i \in \mathcal{C}, \quad \forall j \in \mathcal{N}_i, \tag{19g}$$

where constraints (19b), (19c), and (19d) represent the maximum and minimum limits of prosumers' power set points, bus voltage, and line power flow, respectively. Eq. (19e) is the reciprocity coupled constraint between prosumers i and j. Eqs. (19f) and (19g) state that $p_{i,j}$ is positive when prosumer i is a producer and j is a consumer, and vice-versa. The optimization problem (19) is a strongly convex (proof is given in Appendix B), which can readily be solved using a conventional solver. However, a central coordinator may be required in such approach, wherein the prosumers may need to share their cost function coefficients and energy generation and consumption profiles, which could raise privacy issues and the prosumers may not be willing to disclose these information. Considering that, a privacy-preserving distributed optimization problem is formulated in the following section, and the closed-form solution is derived afterwards.

Remark 2 *For a feasible solution in (19), the maximum generation limit in a given system should be higher than the minimum consumption limit; moreover, the line power flow capacity should wisely be designed.*

This article has been accepted for publication in a future issue of this journal, but has not been fully edited. Content may change prior to final publication. Citation information: DOI 10.1109/TSG.2021.3063960, IEEE Transactions on Smart Grid

IV. Proposed P2P Energy Trading Approach

In this section, the centralized trading problem is decomposed into multiple sub-problems by distributed ADMM algorithm and solved using an iterative approach. A closed-form solution is also derived using first-order method.

A. ADMM-based Solution

As there are no time-coupling constraints in the presented system, we will drop subscript t in rest of the paper. The ADMM algorithm is an effective optimization approach with coupled constraints. In (19e), it can be seen that the power $p_{i,j}$ is coupled between prosumer i and j, which is in multi-block structure. This can be modified into a two-block subproblem and can be solved using standard ADMM with an auxiliary variable ρ. The best known rate of convergence for the standard ADMM algorithm is $\mathcal{O}(1/k)$ [35]–[37], where k is the iteration number. Using various accelerated ADMM algorithms, faster convergence rate of order $\mathcal{O}(1/k^2)$ can be obtained which is proven to be optimal [38]–[40]. In this paper, instead of standard ADMM, F-ADMM [41] algorithm that offers convergence rate of order $\mathcal{O}(1/k^2)$ was adopted with a predictor-corrector type acceleration step, which is stable for the cases with the strongly convex objective functions.

The coupled constraint (19e) can be reformulated as

$$\rho_{i,j} = p_{i,j}, \qquad \forall i \in \mathcal{N}, \quad \forall j \in \mathcal{N}_i, \tag{20a}$$
$$\rho_{i,j} + \rho_{j,i} = 0, \quad \forall i \in \mathcal{N}, \quad \forall j \in \mathcal{N}_i, \tag{20b}$$
$$\rho_{j,i} = p_{j,i}, \qquad \forall i \in \mathcal{N}, \quad \forall j \in \mathcal{N}_i. \tag{20c}$$

Defining $\pi_{i,j}$ as the dual variables associated with (20a), the augmented Lagrangian for (19) can be written as:

$$\mathcal{L}(p_{i,j}, \pi_{i,j}, \rho_{i,j}) = \sum_{i\in\mathcal{N}} \Bigg[u_i(\hat{p}_i) + n_i(\hat{p}_i) - r_i(\hat{p}_{i,t}) + \sum_{j\in\mathcal{N}_i} \left\{ \pi_{i,j}\big(\rho_{i,j} - p_{i,j}\big) + \frac{\eta}{2}\big(\rho_{i,j} - p_{i,j}\big)^2 \right\} \Bigg], \tag{21}$$

where non-zero η is a well-defined positive penalty parameter for the constraint (20a). The ADMM is an iterative approach; it involves solving three different sub-problems in each iteration. Specifically, the first sub-problem ($\mathcal{S}_{\mathcal{P}1}$) associates with solving the local problem based on the current dual variable $\pi_{i,j}$, and auxiliary variable $\rho_{i,j}$. At k-th iteration, each prosumer solves the following local optimization problem to determine the traded power $p_{i,j}^{k+1}$ given that $\pi_{i,j}^k$ and $\rho_{i,j}^k$ as:

$$\begin{aligned} \min_{p_{i,j}} \quad & u_i(\hat{p}_i) + n_i(\hat{p}_i) - r_i(\hat{p}_{i,t}) \\ & + \sum_{j\in\mathcal{N}_i} \left\{ \pi_{i,j}^k\big(\rho_{i,j}^k - p_{i,j}\big) + \frac{\eta}{2}\big(\rho_{i,j}^k - p_{i,j}\big)^2 \right\}, \\ \text{s.t.} \quad & (19b), (19c), (19d), (19f), (19g). \end{aligned} \tag{22}$$

In second sub-problem $\mathcal{S}_{\mathcal{P}2}$, the prosumers update the auxiliary variables $\rho_{i,j}^{k+1}$ based on the solution $p_{i,j}^{k+1}$ of $\mathcal{S}_{\mathcal{P}1}$ and constraint (20b), which can be given as:

$$\begin{aligned} \min_{\rho_{i,j}} \quad & \sum_{i\in\mathcal{N}} \sum_{j\in\mathcal{N}_i} \left\{ \pi_{i,j}^k(\rho_{i,j} - p_{i,j}^{k+1}) + \frac{\eta}{2}(\rho_{i,j} - p_{i,j}^{k+1})^2 \right\}, \\ \text{s.t.} \quad & (20b). \end{aligned}$$

It can be noticed that the auxiliary variables are only coupled between each pair of trading prosumers i and j. Therefore, the optimization problem in $\mathcal{S}_{\mathcal{P}2}$ can be reformulated as:

$$\min_{\rho_{i,j},\rho_{j,i}} \left\{ \pi_{i,j}^k(\rho_{i,j} - p_{i,j}^{k+1}) + \frac{\eta}{2}\big(\rho_{i,j} - p_{i,j}^{k+1}\big)^2 \right\} + \left\{ \pi_{j,i}^k(\rho_{j,i} - p_{j,i}^{k+1}) + \frac{\eta}{2}(\rho_{j,i} - p_{j,i}^{k+1})^2 \right\}, \tag{24a}$$
$$\text{s.t.} \quad (20b). \tag{24b}$$

Based on solutions $p_{i,j}^{k+1}$ and $\rho_{i,j}^{k+1}$ obtained by solving the sub-problems $\mathcal{S}_{\mathcal{P}1}$ and $\mathcal{S}_{\mathcal{P}2}$, respectively, the third sub-problem $\mathcal{S}_{\mathcal{P}3}$ updates the dual variable $\pi_{i,j}^{k+1}$, which can be given by using standard ADMM as:

$$\pi_{i,j}^{k+1} = \pi_{i,j}^k + \eta(\rho_{i,j}^{k+1} - p_{i,j}^{k+1}). \tag{25}$$

Remark 3 *If flexible loads and energy storage systems are considered in the optimization, the time coupling constraints should be considered in (19) which will appear in (22) as well. In that case, closed form solution for $p_{i,j}$ which is derived in the following sub-sections may not easily be achievable. Thus, any convex optimization solvers such as Matlab CVX, IBM ILOG CPLEX, Gurobi, and so on can be utilized to solve (22). The solution for $\rho_{i,j}$ in (32) remains the same.*

B. Closed-form Solutions

1) Closed-form solution to the Sub-problem $\mathcal{S}_{\mathcal{P}1}$: The strongly convex optimization problem $\mathcal{S}_{\mathcal{P}1}$ in (22) is a second-order problem to be solved using Lagrangian-based approach. In this case, the Lagrangian equation can be written as:

$$\begin{aligned} \mathcal{L}(p_{i,j},\pi_{i,j}, \boldsymbol{\tau}, \boldsymbol{\phi}) &= u_i(\hat{p}_i) + n_i(\hat{p}_i) - r_i(\hat{p}_{i,t}) \\ &+ \sum_{j\in\mathcal{N}_i} \left\{ \pi_{i,j}(\rho_{i,j} - p_{i,j}) + \frac{\eta}{2}\big(\rho_{i,j} - p_{i,j}\big)^2 \right\} \\ &+ \sum_{i=1}^{N} \tau_{i,p}(p_i - p_i^{\max}) - \sum_{i=1}^{N} \phi_{i,p}(p_i - p_i^{\min}) \\ &+ \sum_{i=1}^{N} \tau_{i,v}(v_i - v_i^{\max}) - \sum_{i=1}^{N} \phi_{i,v}(v_i - v_i^{\min}) \\ &+ \sum_{l=1}^{N} \tau_{l,f}(f_l - f_l^{\max}) - \sum_{l=1}^{N} \phi_{l,f}(f_l - f_l^{\min}), \end{aligned} \tag{26}$$

where $\boldsymbol{\tau} = \{\tau_{i,p}, \tau_{i,v}, \tau_{l,f}\}$ and $\boldsymbol{\phi} = \{\phi_{i,p}, \phi_{i,v}, \phi_{l,f}\}$ are the local Lagrangian variables $\forall i \in \mathcal{N}, \forall l \in \mathcal{L}$ that define the boundaries for the maximum and minimum power set points, voltage, and line power flow limits. With this definition, the first-order optimality conditions of the relaxed problem, given by the Karush–Kuhn–Tucker (KKT) conditions, are for all the prosumers as:

$$\nabla_{p_{i,j}} \mathcal{L}(p_{i,j}, \pi_{i,j}, \boldsymbol{\tau}, \boldsymbol{\phi}) = 0, \tag{27}$$

which gives

$$\begin{aligned} &2\alpha_i p_{i,j} + \beta_i + \lambda_{i,j} - \omega_{i,j} - \pi_{i,j} - \eta(\rho_{i,j} - p_{i,j}) + \tau_{i,p} - \\ &\phi_{i,p} + \sum_{b=1}^{N} \mathbf{R}_{b,i}(\tau_{b,v}^k - \phi_{b,v}^k) + \sum_{l=1}^{N} \mathbf{A}_{l,i}(\tau_{l,f}^k - \phi_{l,f}^k) = 0. \end{aligned} \tag{28}$$

In (28), $\mathbf{R}$ and $\mathbf{A}$ matrices should be adopted from (5) and (6), respectively. In each successful negotiation between producer i and consumer j, the target power set point can be given by solving (28) as:

$$p_{i,j}^{k+1} = \frac{\pi_{i,j}^k - \lambda_{i,j} + \omega_{i,j} - \tau_{i,p}^k + \phi_{i,p}^k - \beta_i + \eta\rho_{i,j}^k - \mathcal{G}_i^k}{2\alpha_i + \eta}, \tag{29a}$$

$$\mathcal{G}_i^k = \sum_{b=1}^{N} \mathbf{R}_{b,i}(\tau_{b,v}^k - \phi_{b,v}^k) + \sum_{l=1}^{N} \mathbf{A}_{l,i}(\tau_{l,f}^k - \phi_{l,f}^k). \tag{29b}$$

It can be noticed that $\mathcal{G}_i$ in (29) contains the terms related to the bus voltages and line power flow constraints. We are assigning an agent named as network manager (*NM*), who is responsible to solve (29b) based on the power set points provided by the prosumers. Considering the constraint (19f) and (19g), the complete solution can be derived as:

$$p_{i,j}^{k+1} = \max\left\{0, p_{i,j}^{k+1}\right\}, \qquad \forall i \in \mathcal{P}, \quad \forall j \in \mathcal{N}_i, \tag{30a}$$

$$p_{i,j}^{k+1} = \min\left\{0, p_{i,j}^{k+1}\right\}, \qquad \forall i \in \mathcal{C}, \quad \forall j \in \mathcal{N}_i. \tag{30b}$$

In the next step, the local Lagrangian variables $\boldsymbol{\tau}$ and $\boldsymbol{\phi}$ should be updated taking complementary slackness into account as:

$$\boldsymbol{\tau}^{k+1} = \max\left\{0, \boldsymbol{\tau}^k + \xi_{\mathbf{z}}\big(\mathbf{z}^{k+1} - \mathbf{z}^{\max}\big)\right\}, \tag{31a}$$

$$\boldsymbol{\phi}^{k+1} = \max\left\{0, \boldsymbol{\phi}^k - \xi_{\mathbf{z}}\big(\mathbf{z}^{k+1} - \mathbf{z}^{\min}\big)\right\}, \tag{31b}$$

where $\boldsymbol{\tau} := \{\tau_{i,p}, \tau_{i,v}, \tau_{l,f}\}$, $\boldsymbol{\phi} = \{\phi_{i,p}, \phi_{i,v}, \phi_{l,f}\}$, $\mathbf{z} := \{p_i, v_i, f_l\}$, $\forall i \in \mathcal{N}, \forall l \in \mathcal{L}$; $\mathbf{z}^{\max}$ and $\mathbf{z}^{\min}$ contains the maximum and minimum values of the elements in $\mathbf{z}$, respectively. The optimization step size $\xi_{\mathbf{z}} := \{\xi_p, \xi_v, \xi_f\}$, which are utilized to update corresponding Lagrangian variables $\boldsymbol{\tau}$ and $\boldsymbol{\phi}$. It should be noted that the *NM* determines v_i and f_l using (5) and (6), respectively and updates all $\tau_{i,v}$, $\tau_{l,f}$, $\phi_{i,v}$, and $\phi_{l,f}$. The each prosumer i updates their local Lagrangian variables $\tau_{i,p}$ and $\phi_{i,p}$.

2) Closed-form Solution to the Sub-problem $\mathcal{S}_{\mathcal{P}2}$: By applying Lagrangian approach with first-order KKT conditions in (24), we can obtain the closed form solution for updating $\rho_{i,j}$ as:

$$\rho_{i,j}^{k+1} = -\rho_{j,i}^{k+1} = \frac{\eta(p_{i,j}^{k+1} - p_{j,i}^{k+1}) - (\pi_{i,j}^k - \pi_{j,i}^k)}{2\eta}. \tag{32}$$

C. F-ADMM-based solution to the sub-problem $\mathcal{S}_{\mathcal{P}3}$

F-ADMM algorithm uses a predictor-corrector type acceleration step in the dual variable update step. Therefore, by using F-ADMM algorithm, the dual variable (price signal) $\pi_{i,j}^{k+1}$ can be updated using following steps as:

$$\tilde{\pi}_{i,j}^k = \pi_{i,j}^k + \eta(\rho_{i,j}^{k+1} - p_{i,j}^{k+1}), \tag{33a}$$

$$\mu_i^{k+1} = \frac{1 + \sqrt{1 + 4{\mu_i^k}^2}}{2}, \tag{33b}$$

$$\pi_{i,j}^{k+1} = \tilde{\pi}_{i,j}^k + \frac{\mu_i^k - 1}{\mu_i^{k+1}}(\pi_{i,j}^k - \pi_{i,j}^{k-1}), \tag{33c}$$

where μ_i is the acceleration operator for prosumer i. It should be noted that the bilateral traded power ($p_{i,j}$) and auxiliary variable ($\rho_{i,j}$) should be calculated by using (29a) and (32),

Algorithm 1: Proposed energy trading approach between prosumer i and j in parallel using F-ADMM algorithm.

Input : $\{I^{\max}, \pi_{i,j}^0, \pi_{i,j}^1, \rho_{i,j}^1, \tau_{i,p}^1, \phi_{i,p}^1, \mathcal{G}_i^1, \mu_i^1\}$
Output: $\{p_{i,j}^*, \pi_{i,j}^*\}$

for $k = 1 : I^{\max}$ **do**
- **Prosumer** i:
  - Updates $p_{i,j}^{k+1}$ by (29) and (30).
  - Exchanges $p_{i,j}^{k+1}$ and $p_{j,i}^{k+1}$ with prosumer $j \in \mathcal{N}_i$.
  - Updates $\rho_{i,j}^{k+1}$ by (32).
  - Updates $\pi_{i,j}^{k+1}$ by (33c).
  - Exchanges $\pi_{i,j}^{k+1}$ and $\pi_{j,i}^{k+1}$ with prosumer $j \in \mathcal{N}_i$.
  - Determines total traded power p_i by (17).
  - Transmits p_i to network manager.
  - Updates $\tau_{i,p}^{k+1}$ and $\phi_{i,p}^{k+1}$ by (31).
- **Network Manager**:
  - Receives p_i, $\forall i \in \mathcal{N}$.
  - Updates all $\tau_{i,v}^{k+1}$ $\tau_{l,f}^{k+1}$, $\phi_{i,v}^{k+1}$, and $\phi_{l,f}^{k+1}$ by (31).
  - Calculates $\mathcal{G}_i^{k+1}$, $\forall i \in \mathcal{N}$ by (29b).
  - Transmits $\mathcal{G}_i^{k+1}$ to prosumer i.

end

respectively, through the accelerated price signal $\pi_{i,j}$ from (33c). However, the paired prosumers i and j share only the traded power $p_{i,j}$ and the price $\pi_{i,j}$ in each iteration. The prosumers do not share total power generation or consumption profile with their fellow prosumers but a partial quantity only; therefore, the prosumers' privacy is not violated. The proposed energy trading scheme is summarized in Algorithm 1. It is worth noting that all the computations and updates in each step are parallel between the prosumers.

D. Convergence Error and Stopping Criterion

The overall convergence error for the designed algorithm can be calculated as:

$$\delta^k = \sqrt{{\delta_1^k}^2 + ... + {\delta_n^k}^2 + ... + {\delta_7^k}^2}, \tag{34}$$

where $\delta_n^k = \left\|\hat{y}_n^k - \hat{y}_n^{k-1}\right\|_2$, $\|A\|_2$ represents the L_2 norm of A, and $\hat{y} := \{\mathbf{p}, \boldsymbol{\tau}_p, \boldsymbol{\tau}_f, \boldsymbol{\tau}_v, \boldsymbol{\phi}_p, \boldsymbol{\phi}_f, \boldsymbol{\phi}_v\}$. Individual convergence error δ_i can also be calculated based on the available information of $\hat{y}$ at each end. In this paper, the stopping condition for the algorithm was $\delta_i \leq 10^{-3}$. The other stopping criterion for the producers, consumers, and the *NM* can be considered as in [13], [25].

Theorem 1 *The proposed energy trading algorithm converges at a rate of $\mathcal{O}(1/k^2)$ if there is a feasible solution for $p_{i,j}$ in (19) and the utility function is strongly convex with coefficient $\alpha_i > 0$.*

Proof: The proof of theorem 1 is given in Appendix B.

Remark 4 *Although the proposed methodology is designed for P2P energy trading in tree topology radial networks, it can also be implemented in meshed networks with reformulated network constraints. Since the electrical structure is typically fixed during energy trading, the network manager (NM) can easily select the network topology before the market clearing process. In meshed networks, the NM can consider decoupled power flow (DCPF) method from [42] to manage the physical network constraints. The details are given in Appendix C.*

This article has been accepted for publication in a future issue of this journal, but has not been fully edited. Content may change prior to final publication. Citation information: DOI 10.1109/TSG.2021.3063960, IEEE Transactions on Smart Grid

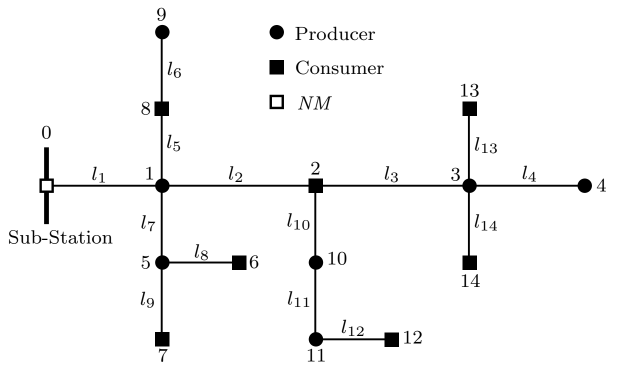

Fig. 2: Prosumer-centric IEEE 15-bus distribution system. l_x represents line x and *NM* is the network manager.

V. Simulation Result and Analysis

This section presents the analysis on the simulation result with various case studies, which demonstrates the aspects of the proposed energy trading approach.

A. Simulation Setup

A standard IEEE 15-bus system that consists of 14 prosumers (7 prosumers and 7 consumers) shown in Fig. 2 is considered in the simulation. It was assumed that the prosumers have rooftop PV panels installed. The bus 0 is the slack bus where the *NM* agent is located, who is responsible for preventing any network constraint violation by solving (29b) for $\mathcal{G}_i$ when the prosumers negotiate in the trading. The energy producer agents are located in bus $1, 3, 4, 5, 9, 10$, and 11 and the consumer agents are positioned in the remaining buses. The network data, such as branch resistance and reactance values, are adopted from [43]. The optimization parameters are randomly generated in an interval. The cost function parameters for producer are considered to be $\alpha_i \in [0.26,\ 0.78]$ ¢/kWh^2, $\beta_i \in [2.6,\ 6.5]$ ¢/kWh. Similarly, $\alpha_i \in [0.9,\ 1.25]$ ¢/kWh^2, $\beta_i \in [9.1,\ 16.9]$ ¢/kWh for the consumer agents. The upper and lower power limits for producer agents are selected to be $p_i^{\max} \in [10, 30]$ kW and $p_i^{\min} \in [5, 7]$ kW, respectively. Likewise, the upper and lower limit for the consumer agents are assumed to be $p_i^{\max} \in [-7, -5]$ kW and $p_i^{\min} \in [-30, -10]$ kW. The reactive powers were assumed to be 80% of the bus injected real powers. The initial values of the power and price are set to $p_{i,j}^1 = 0$ kW, and $\pi_{i,j}^0 = \pi_{i,j}^1 = 0$ ¢/kWh, respectively. The $\mathcal{G}_i^1$ is set to 0, $\forall i$. It was considered that the energy buying price from the grid is 15 ¢/kWh and selling price to the grid is 5 ¢/kWh. The reputation function parameter $c = 0.1$ ¢/kWh and per unit service charge $\gamma = 0.01$ ¢/Ω.kWh. The prosumers are aware of this prices and settle the bilateral trades in between these prices so that both the producers and consumers can maximize their profits. Although the simulation was performed only for one hour, the proposed strategy can readily be applied for multi-time step systems. The simulations were performed with MATLAB 2019. To evaluate the effectiveness of the proposed algorithm, six case studies were conducted. It should be noted that the product differentiation and network utilization fees which are briefly analyzed in *Case VI*, are not considered for *Case I-Case V*.

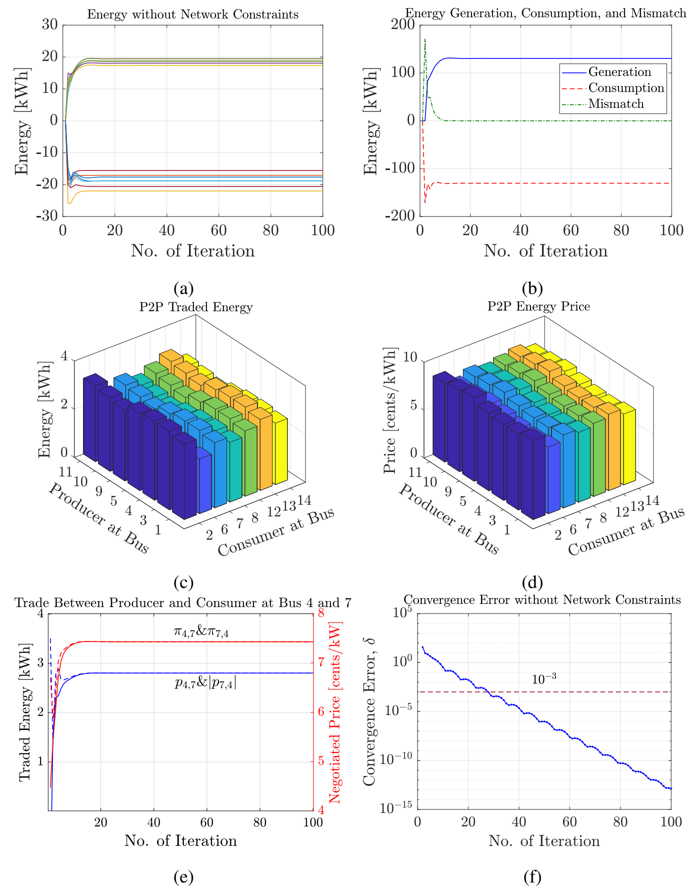

Fig. 3: IEEE 15-bus distribution system analysis without network constraints in the energy trading: (a) Power injection in different buses (p_i) by the prosumers, (b) Total energy generation, consumption, and balance, (c) Traded energy between the prosumers, (d) Traded energy prices between the prosumers, (e) Evolution of traded energy and negotiated price between prosumers at bus 4 and 7, and (f) Convergence error (δ).

B. Case I: Energy Trading Without Network Constraints

This case study was conducted without considering the bus voltage and line power flow constraints in the bilateral energy-trading optimization problem described in Section IV. In this case, the traded energy set points can be determined by simply putting $\mathcal{G}_i = 0$ in (29b). The results obtained from the proposed algorithm is shown in Fig. 3. It can be seen from Fig. 3a that the energy set points of all the prosumers reached steady-states in less than 30 iterations resulting in zero energy mismatch as depicted in Fig. 3b. The amount of total traded energy in the system is 130.4 kWh. The traded energy and the settled prices are presented in Figs. 3c and 3d. It can be noticed that the negotiated energy prices are between 5 ¢/kWh and 15 ¢/kWh, which indicates that the prosumers can maximize their profits by trading energy among themselves rather than trading with the main grid. To show the evolution of traded and the negotiated price, we selected the producer at bus 4 and consumers at bus 7, which are delineated in Fig. 3e. It is easily observable that both the energy and price match within a few iterations, which accelerates the convergence speed of the proposed bilateral energy trading algorithm. The evolution of the convergence error in Fig. 3f indicates that the proposed algorithm convergences when $k = 27$. The total computation time was found less than 1 second, although it may vary

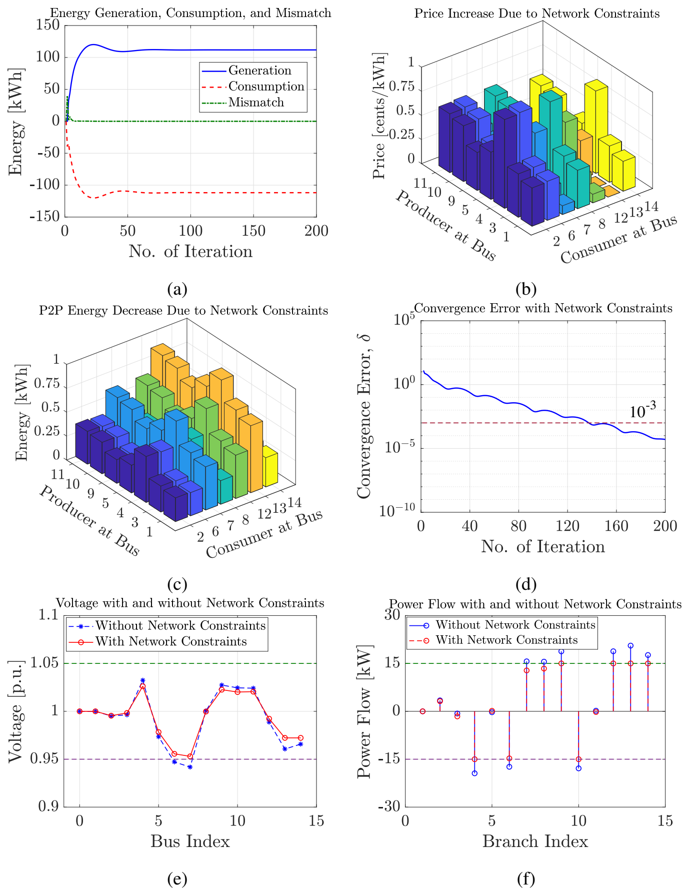

Fig. 4: IEEE 15-bus distribution system analysis with network constraints: (a) Total energy generation, consumption, and balance, (b) Increase in negotiated price between the prosumers, (c) Decrease in traded energy between the prosumers, (d) Convergence error (δ), (e) Bus voltages with and without considering network constraints, and (f) Power flow in different brunches with and without considering network constraints.

slightly in different computation devices.

C. Case II: Energy Trading Considering Network Constraints

In this case, the proposed market clearing algorithm was simulated under the network influence with the bus voltage and line power flow constraints, as described in (19). The obtained results are presented in Fig. 4. Noticeably, the total amount of traded energy (111.8 kWh) is lower than the *Case I* as illustrated in Fig. 4a. This is due to the increase in the negotiated price (Fig. 4b), which eventually results in the diminution of traded energy as in Fig. 4c. It indicates that the prosumers are able to manage their trade, respecting the system constraints. Fig. 4d depicts that the convergence criterion ($\delta \leq 10^{-3}$) is fulfilled when $k = 133$, which is a bit higher than that in *Case I*. This is due to the voltage and line power flow constraints imposed in the optimization problem.

One of the major contributions of this paper is to consider the network constraints in the market-clearing approach so that the power lines are not overly congested and the bus voltages do not violate the standard at the same time, which is $\pm 5\%$ of 1 per unit (p.u.). It was assumed in this case that the maximum and minimum line power flows are 15 kW and -15 kW, respectively. These limits may vary according to the system design preference. However, it is evident from Fig. 4e

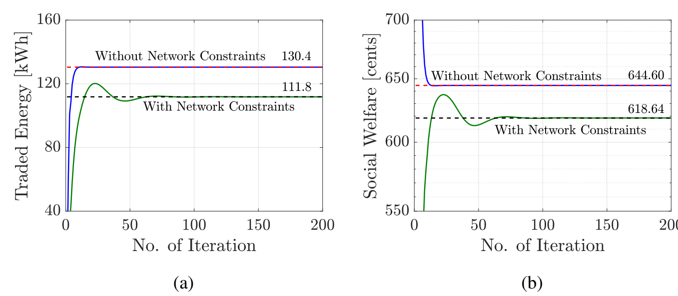

Fig. 5: Optimality analysis of the proposed scheme compared to centralized approach considering with and without network constraints: (a) Total traded energy in the system, and (b) Total social welfare of the system. The dashed lines represent centralized result and the solid lines indicates the results obtained using proposed approach.

that the voltage in the buses 6 and 7 violate the minimum voltage limit of 0.95 p.u. while the network constraints were not considered. The voltages stay inside the limits of 0.95 p.u. to 1.05 p.u. when the voltage constraints were imposed on the optimization problem. In this regard, the amount of power injections in different buses were reduced. It is noticeable from Fig. 4f that the line power flow constraints are also satisfied in the proposed P2P energy trading approach, which may protect the power line from being over-congested in a given system. It should be noted that the violation of these constraints may adversely affect the reliability and stability of a distribution system. In that context, the proposed trading approach will enhance the power system performance in P2P energy sharing.

D. Case III: Comparison With Centralized Approach

This case study describes the optimality analysis of the proposed algorithm comparing with the centralized approach, which is demonstrated in Fig. 5. It can be seen in Fig. 5a that the total amount of traded energy with and without considering network constraints was found as same as the values in the centralized approach within a certain number of iterations, which are 111.8 kW and 130.4 kW, respectively. This is also true for the total social welfare of the system (as shown in Fig. 5b), which were 644.60¢ and 618.64¢ without and with considering network constraints, respectively. These indicate that the individual traded power quantities between all the prosumer pairs i and j ($p_{i,j}$) also reach the optimal points within certain number of iterations with and without considering network constraints. It is worth noting that this case study justified the optimality of the proposed distributed P2P energy trading algorithm in Section IV with compared to the centralized optimization problem (19).

E. Case IV: Comparison with Existing Approaches without Considering Network Constraints

The performance of the proposed algorithm is compared with the two existing distributed market-clearing approaches in a system of 7 prosumers (4 producers and 3 consumers). We are naming the approaches as algorithm $A2$ (standard ADMM), algorithm $A3$ [25], and algorithm $A4$ [13]. In algorithm $A2$, the predictor-corrector type acceleration step was excluded which transforms the F-ADMM into the standard

This article has been accepted for publication in a future issue of this journal, but has not been fully edited. Content may change prior to final publication. Citation information: DOI 10.1109/TSG.2021.3063960, IEEE Transactions on Smart Grid

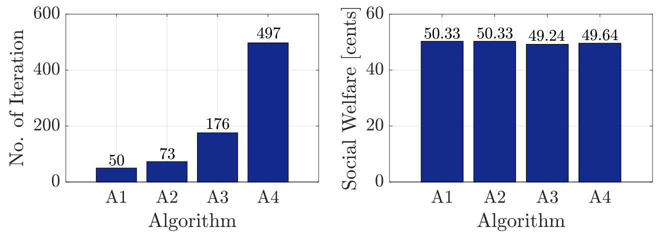

Fig. 6: Comparison with existing algorithms. $A1$: proposed approach, $A2$: standard ADMM, $A3$: algorithm [25], and $A3$: algorithm [13].

ADMM. The algorithm $A3$ described a first-order primal-dual gradient method, whereas the algorithm $A4$ presented a relaxed consensus+innovation method. In this case, the optimization parameters such as cost function coefficients, maximum, and minimum power limits are adopted from [25]. The same convergence criterion is also considered from the respective papers. In this case, bus voltage and line power flow constraints were not considered in order to have a generalized optimization problem. The future power system is apprehended to be more distributed with the participation of numerous prosumers. Therefore, the market-clearing approaches should be faster not only in respect of computation time but also in the number of iterations. In that regard, the performance of the proposed approach was compared concerning the number of required iteration to converge, along with the total social welfare (¢) of the system, as portrayed in Fig. 6. It can be seen that the developed approach takes fewer iterations to converge. The proposed approach takes only 50 iterations, whereas algorithms $A2$, $A3$, and $A4$ take 73, 176, and 497 iterations, respectively. The social welfare of the system considering the proposed trading approach is 50.33¢, wherein it is 49.24¢ and 49.64¢ for approaches $A2$ and $A3$. The social welfare using algorithm $A2$ is also same as the algorithm $A1$. Another important feature of an energy trading approach is the computation time, which depends on the number of iterations and the solution approach. The proposed approach was solved applying first-order KKT conditions on relaxed Lagrangian problem as in algorithms $A2$, $A3$, and $A4$. This indicates that the proposed scheme will take less computation time compared to these existing approaches since it takes fewer iterations to converge. It is worth noting that the proposed approach converges in less than 1 second, although it may vary a bit in various computing devices.

F. Case V: Scalability Analysis

This case study analyzes the scalability of the proposed approach for a various number of prosumers and different distribution networks. The proposed algorithm allows more prosumers to participate in the energy tradings within a tolerable computation time. Two scenarios were considered: without network constraints having 100-1000 prosumers and with network constraints in IEEE 33, 69, 85, and 141 bus systems occupied with 32, 68, 84, and 140 prosumers. In the distribution systems, bus 0 is the slack bus and the remaining buses are prosumers. For simplicity, it was considered that there was an equal number of producers and consumers in the system. The position of the prosumers was picked randomly. The line power flow limits were arbitrarily selected. The presented optimization model was simulated for about 1000 times in each sub-scenarios of both of the scenarios. It can be noticed that the ratio of the required iterations to the number of prosumers is a bit higher in the second scenario since two additional network constraint sets were considered. It is also noticeable from Figs. 7a and 7b that the number of iterations may increase if the number of prosumers in the system is increased. However, if the tuning parameters are properly set, the proposed energy trading algorithm may converge in less than 300 iterations for all the systems. The computation time, when the proposed scheme was applied in IEEE 33, 69, 85, and 141 bus systems, is presented in Fig. 7c. Although a system with higher number of prosumers may require more computation time, it may be considered acceptable even if 5 minutes ahead of market operation is taken into account. It is important to be mentioned in this case study that the bus voltages in each distribution system also remained within the safe limits, as depicted in Fig. 7d.

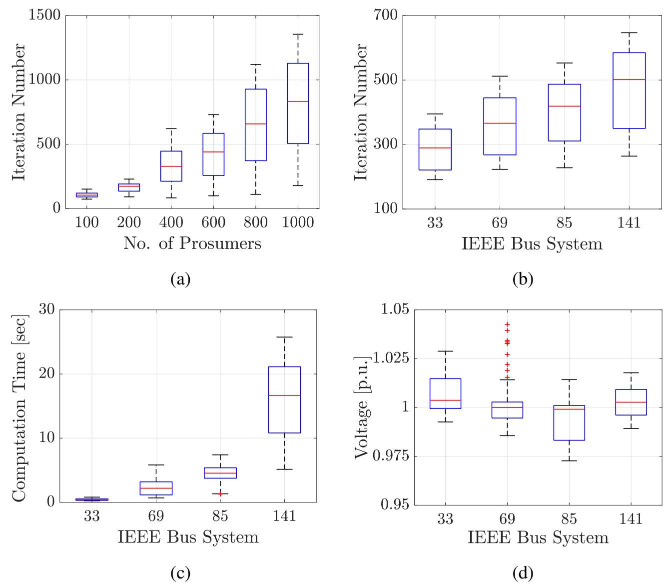

Fig. 7: Saclability analysis of the proposed algorithm. Sub-figure (a) is plotted without considering network constraints and remaining are plotted with considering network constraints. (a) Number for required iterations, (b) Number for required iterations, (c) Computation time, and (d) Bus voltages, when the network constraints were considered in IEEE 33, 69, 85 and 141 bus systems with 32, 68, 84, and 140 prosumers, respectively.

G. Case VI: Analysis of Product Differentiation and Network Utilization Fees

This case study presents the impact of mutual reputation index (MRI) and network utilization fee (NUF) in the bilateral energy trading.

1) Reputation-based Product Differentiation: Figs. 8-9 show the obtained results considering MRI in energy trading. We considered two scenarios for energy transactions at different values of MRI. Scenario 1 represents the trading between producer at bus 1 and consumer at bus 8, and scenario 2 shows trading between producer at bus 2 and consumer at bus 3. One can expect that the higher MRI should lead to a higher willingness of market participants in P2P energy trading that can be justified from Fig. 8. It can be seen that the negotiated

This article has been accepted for publication in a future issue of this journal, but has not been fully edited. Content may change prior to final publication. Citation information: DOI 10.1109/TSG.2021.3063960, IEEE Transactions on Smart Grid

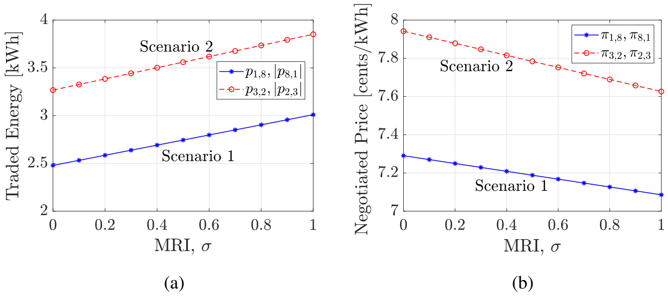

Fig. 8: Impact of MRI in the P2P bilateral trading: (a) Traded energy, and (b) Negotiated price.

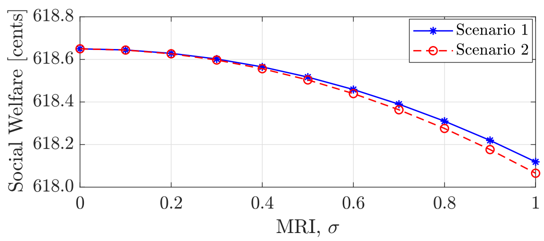

Fig. 9: Total social welfare of the system in scenarios 1 and 2 for different values of MRI.

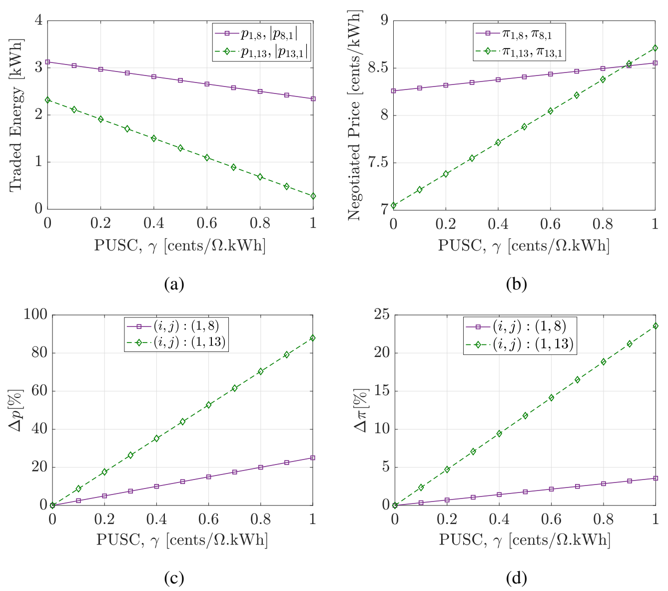

Fig. 10: Impact of network utilization fees in P2P bilateral trading: (a) Traded energy between producer and consumer pairs (1,8) and (1,13), (b) Negotiated price between producer and consumer pairs (1,8) and (1,13), (c) Relative change in traded energy ($\Delta \boldsymbol{p}$), and (d) Relative change in negotiated prices ($\Delta \boldsymbol{\pi}$). PUSC is the per unit service charge.

prices between the producers and consumers decrease, and at the same time, the amount of traded energy increases when the MRI increases. It is noteworthy that the inclusion of MRI in bilateral trading influences the traders' willingness but may not significantly affect their overall social welfare. Fig. 9 shows that the total social welfare decreased by less than 0.6¢ in both the scenarios, which can be considered as negligible.

2) Network Utilization Fee (NUF): In this sub-case, the NUF was considered in energy tradings between the producer and consumer pairs at buses (1, 8), and (1, 13). The obtained results are shown in Fig. 10. It is perceptible from Figs. 10a and 10b that the amount of traded energy decreases and the negotiated price increases when the per-unit service charge (PUSC) increases, but the rate of change varies in trading pairs $(1,8)$ and $(1,13)$. The relative changes in traded energy (Δp) and negotiated price ($\Delta \pi$) compared to the case without considering PUSC (i.e., $\gamma = 0$) are presented in Figs. 10c and 10d, respectively. It can easily be noticed that the rate of changes in Δp and $\Delta \pi$ are higher in the case of trading between producer 1 and consumer 13 than the trading between producer 1 and consumer 8, which can be interpreted from the perspective of net electrical distance $d_{i,j}$. It should be noted from Fig. 2 that the net electrical distance between buses 1 and 8 is smaller than the distance between buses 1 and 13, $d_{1,8} < d_{1,13}$. This analysis indicates that the energy traders are inclined to trade more energy with the closer traders than the furthest. Thus, in turn, imposing NUF in energy trading may reduce network power loss since more energy needs to be transported to a shorter distance.

VI. Conclusion and Future Research

In this paper, a scalable P2P energy trading approach was proposed for prosumer-centric transactive energy systems using an F-ADMM-based optimization algorithm. A closed-form solution was derived to reduce the computation time. The proposed scheme, with no central coordinator required in transactions, allows numerous prosumers to settle the market by sharing minimal information among themselves. The proposed scheme provides a feasible solution and converges faster. The convergence was verified through simulations. The presented energy trading model was applied to IEEE 15-bus standard distribution network and justified its effectiveness. Besides, reputation-based product differentiation that measures the market participants' willingness to trade with particular traders was introduced. Moreover, the power line congestion and voltage management were considered in the pricing model to enhance reliability and stability in the energy market with P2P energy sharing. Although the proposed methodology was applied in tree-topology distribution networks in simulations, it is not limited to them. It was also demonstrated that the proposed approach can be adopted for mesh network as well. Moreover, our work can further be extended to address the following issues. Firstly, this paper excludes network power losses which can be included in the energy pricing. The uncertainty of solar irradiance and load demand can also be considered. Secondly, in this paper, energy traders were supposed to utilize synchronous communication without transmission delay. Thus, energy trading with asynchronous communication and delay can be potential research topics. Thirdly, distributed ledger technology such as blockchain can be incorporated in the system to ensure the transparency of transactions [44].

Appendix

A. Assumptions of Problem

Following assumptions are considered for this paper.

Assumption 1 The optimization problem in (19) has a nonempty set of optimal solutions, i.e., $\Pi^* \neq \emptyset$, where Π^* is the optimal solution set of problem (19).

This article has been accepted for publication in a future issue of this journal, but has not been fully edited. Content may change prior to final publication. Citation information: DOI 10.1109/TSG.2021.3063960, IEEE Transactions on Smart Grid

Assumption 2 For any prosumer $i \in \mathcal{N}$, the local function $f_i(p_{i,j})$ is coercive and strongly convex such that $||p_{i,j}|| \rightarrow \infty$ cause that $||f_i(p_{i,j})|| \rightarrow \infty$, where $f_i(p_{i,j}) = u_i(\hat{p}_{i,t}) + n_i(\hat{p}_{i,t}) - r_i(\hat{p}_{i,t})$ and $||.||$ denotes the Euclidean norm.

Assumption 3 Each objective function f_i is strongly convex and differentiable with Lipschitz continuous, i.e., for any prosumers $i \in \mathcal{N}$, $\forall x_1, x_2 \in \mathbb{R}$, the following inequalities holds

$$||g_i(x_1) - g_i(x_2)|| \leq L||x_1 - x_2||,$$
$$f_i(x_1) - f_i(x_2) \leq g_i(x_1)^T(x_1 - x_2) - \frac{\psi}{2}||x_1 - x_2||^2.$$

where g_i is the gradient of f_i, L is the Lipschitz constant, ψ is a positive constant, and $||.||$ denotes the Euclidean norm.

B. Proof of Theorem 1

The F-ADMM algorithm converges at a rate of $\mathcal{O}(1/k^2)$ if the objective function is strongly convex [41]. Let us recall the objective function from (19) as:

$$f_i(p_{i,j}) = \sum_{t\in\mathcal{T}}\sum_{i\in\mathcal{N}} u_i(\hat{p}_{i,t}) + n_i(\hat{p}_{i,t}) - r_i(\hat{p}_{i,t}), \tag{36}$$

At a given time step $t \in \mathcal{T}$, the second derivative of $f_i(p_{i,j})$ with respect to $p_{i,j}$ gives

$$f_i''(p_{i,j}) = 2\alpha_i, \tag{37}$$

Since $\alpha_i > 0$ then $f_i''(p_{i,j}) > 0$, which indicates that the objective function in (19) is strongly convex. Therefore, upon wisely setting the steps sizes and penalty parameters, the proposed energy trading solution using F-ADMM will converge at a rate of $\mathcal{O}(1/k^2)$ and give a feasible solution under the assumptions made in Appendix A, which concludes the proof of *Theorem 1*. The detailed convergence proof for F-ADMM algorithm can be found in [41].

C. Energy Trading Problem Reformulation for Mesh Networks

Consider a mesh power network denoted by a set of buses $\mathcal{N}_\mathcal{B} := \{1, 2, ..., N\}$ and a set of line segments $\mathcal{L} := \{l \rightarrow (i,j)\} \subseteq \mathcal{N}_\mathcal{B} \times \mathcal{N}_\mathcal{B}$. In such networks, decoupled power flow (DCPF) can be considered, which gives [42]

$$\boldsymbol{\theta} = \mathbf{B}^{-1}\mathbf{p} = \mathbf{S}\mathbf{p}, \tag{38a}$$

$$\mathbf{B} = [b_{i,j}]; \quad b_{i,j} = -\frac{1}{x_{i,j}}; \quad b_{i,i} = \sum_{j=1}^{N}\frac{1}{x_{i,j}}, \tag{38b}$$

where $\mathbf{S} := \mathbf{B}^{-1}$, $\mathbf{p}$ and $\boldsymbol{\theta}$ are the vectors of nodal injections and phase angles for buses $1, 2, ..., N$. The power flow from bus i to j for DCPF can be given by [42]

$$P_{i,j} = \frac{1}{x_{i,j}}(\theta_i - \theta_j); \quad \text{for } i,j = 1,2,...,N; \ i \neq j, \tag{39}$$

where $x_{i,j}$ is the reactance between bus i and j, θ_i and θ_j are the voltage phase angles on the bus i and j. Utilizing (38a), the power flows in (39) can be written in the vector form as:

$$\mathbf{P} = \mathbf{M}\boldsymbol{\theta} = \mathbf{M}\mathbf{B}^{-1}\mathbf{p} = \mathbf{H}\mathbf{p} \tag{40}$$

where $\mathbf{H} = \mathbf{M}\mathbf{B}^{-1}$ and $\mathbf{M}$ is a $|\mathcal{L}| \times |\mathcal{N}_\mathcal{B}|$ graph incidence matrix. The entries of $\mathbf{M}$ are defined as $\mathbf{M}_{l,i} = 1/x_l$ if line l leaves i and $\mathbf{M}_{l,i} = -1/x_l$ if line l enters i, where x_l is the reactance of line $l \rightarrow (i,j)$. Now the new constraints of $\boldsymbol{\theta}$ should be considered besides constraints of $\mathbf{P}$ in the optimization model as:

$$\boldsymbol{\theta}^{\min} \leq \boldsymbol{\theta} \leq \boldsymbol{\theta}^{\max}, \tag{41a}$$
$$\mathbf{P}^{\min} \leq \mathbf{P} \leq \mathbf{P}^{\max}, \tag{41b}$$

The update rule for $\mathcal{G}_i$ in (29b) by the network manager can be written as:

$$\mathcal{G}_i^k = \sum_{b=1}^{|\mathcal{N}_\mathcal{B}|}\mathbf{S}_{b,i}(\tau_{b,\theta}^k - \phi_{b,\theta}^k) + \sum_{l=1}^{|\mathcal{L}|}\mathbf{H}_{l,i}(\tau_{l,f}^k - \phi_{l,f}^k). \tag{42}$$

If bus i is the reference bus then $\theta_i^{\min} = \theta_i^{\max} = 0$. The Lagrangian variables $\tau_{i,\theta}$, $\phi_{i,\theta}$, $\tau_{l,f}$, and $\phi_{l,f}$ should updated similar as in (31).

References

[1] M. E. Peck and D. Wagman, "Energy trading for fun and profit buy your neighbor's rooftop solar power or sell your own-it'll all be on a blockchain," *IEEE Spectrum*, vol. 54, no. 10, pp. 56–61, 2017.

[2] J. Guerrero, D. Gebbran, S. Mhanna, A. C. Chapman, and G. Verbič, "Towards a transactive energy system for integration of distributed energy resources: Home energy management, distributed optimal power flow, and peer-to-peer energy trading," *Renewable and Sustainable Energy Reviews*, vol. 132, p. 110000, 2020.

[3] T. Council, "Gridwise transactive energy framework version 1.0," *The GridWise Architecture Council, Tech. Rep*, 2015.

[4] O. Abrishambaf, F. Lezama, P. Faria, and Z. Vale, "Towards transactive energy systems: An analysis on current trends," *Energy Strategy Reviews*, vol. 26, p. 100418, 2019.

[5] F. Rahimi and A. Ipakchi, "Using a transactive energy framework: Providing grid services from smart buildings," *IEEE Electrification Magazine*, vol. 4, no. 4, pp. 23–29, 2016.

[6] W. Tushar, T. K. Saha, C. Yuen, P. Liddell, R. Bean, and H. V. Poor, "Peer-to-peer energy trading with sustainable user participation: A game theoretic approach," *IEEE Access*, vol. 6, pp. 62 932–62 943, 2018.

[7] T. Morstyn, N. Farrell, S. J. Darby, and M. D. McCulloch, "Using peer-to-peer energy-trading platforms to incentivize prosumers to form federated power plants," *Nature Energy*, vol. 3, no. 2, p. 94, 2018.

[8] S. Wu, F. Zhang, and D. Li, "User-centric peer-to-peer energy trading mechanisms for residential microgrids," in *2nd Conference on Energy Internet and Energy System Integration (EI2)*. IEEE, 2018, pp. 1–6.

[9] C. Long, J. Wu, C. Zhang, L. Thomas, M. Cheng, and N. Jenkins, "Peer-to-peer energy trading in a community microgrid," in *PES General Meeting*. IEEE, 2017, pp. 1–5.

[10] Z. Zhang, H. Tang, Q. Huang, and W.-J. Lee, "Two-stages bidding strategies for residential microgrids based peer-to-peer energy trading," in *IEEE/IAS 55th Industrial and Commercial Power Systems Technical Conference (I&CPS)*. IEEE, 2019, pp. 1–9.

[11] T. Liu, X. Tan, B. Sun, Y. Wu, X. Guan, and D. H. Tsang, "Energy management of cooperative microgrids with P2P energy sharing in distribution networks," in *International conference on smart grid communications (SmartGridComm)*. IEEE, 2015, pp. 410–415.

[12] F. Moret, T. Baroche, E. Sorin, and P. Pinson, "Negotiation algorithms for peer-to-peer electricity markets: Computational properties," in *Power Systems Computation Conference (PSCC)*. IEEE, 2018, pp. 1–7.

[13] E. Sorin, L. Bobo, and P. Pinson, "Consensus-based approach to peer-to-peer electricity markets with product differentiation," *IEEE Transactions on Power Systems*, vol. 34, no. 2, pp. 994–1004, 2019.

[14] T. Morstyn and M. McCulloch, "Multi-class energy management for peer-to-peer energy trading driven by prosumer preferences," *IEEE Transactions on Power Systems*, vol. 34, no. 5, pp. 4005–4014, 2019.

[15] M. H. Ullah, A. Alseyast, and J.-D. Park, "Distributed dynamic pricing in peer-to-peer transactive energy systems in smart grid," in *IEEE Power & Energy Society General Meeting (PESGM)*. IEEE, 2020, pp. 1–5.

[16] H. Zhang, Y. Li, D. W. Gao, and J. Zhou, "Distributed optimal energy management for energy internet," *IEEE Transactions on Industrial Informatics*, vol. 13, no. 6, pp. 3081–3097, 2017.

[17] S. Cui, Y.-W. Wang, Y. Shi, and J. Xiao, "An efficient peer-to-peer energy sharing framework for numerous community prosumers," *IEEE Transactions on Industrial Informatics*, vol. 16, no. 12, pp. 7402–7412, 2020.

[18] H. Wang and J. Huang, "Incentivizing energy trading for interconnected microgrids," *IEEE Transactions on Smart Grid*, vol. 9, no. 4, pp. 2647–2657, 2016.

[19] S. Cui, Y.-W. Wang, and J.-W. Xiao, "Peer-to-peer energy sharing among smart energy buildings by distributed transaction," *IEEE Transactions on Smart Grid*, vol. 10, no. 6, pp. 6491–6501, 2019.

[20] K. Anoh, S. Maharjan, A. Ikpehai, Y. Zhang, and B. Adebisi, "Energy peer-to-peer trading in virtual microgrids in smart grids: a game-theoretic approach," *IEEE Transactions on Smart Grid*, vol. 11, no. 2, pp. 1264–1275, 2020.

[21] M. H. Ullah and J.-D. Park, "Peer-to-peer energy arbitrage in prosumer-based smart residential distribution system," in *Energy Conversion Congress and Exposition (ECCE)*. IEEE, 2019, pp. 508–514.

[22] L. Chen, N. Liu, and J. Wang, "Peer-to-peer energy sharing in distribution networks with multiple sharing regions," *IEEE Transactions on Industrial Informatics*, vol. 16, no. 11, pp. 6760–6771, 2020.

[23] J. Kang, R. Yu, X. Huang, S. Maharjan, Y. Zhang, and E. Hossain, "Enabling localized peer-to-peer electricity trading among plug-in hybrid electric vehicles using consortium blockchains," *IEEE Transactions on Industrial Informatics*, vol. 13, no. 6, pp. 3154–3164, 2017.

[24] M. Qi, H. Yang, D. Wang, Y. Luo, S. Zhang, and S. Liao, "Prosumers peer-to-peer transaction decision considering network constraints," in *3rd Conference on Energy Internet and Energy System Integration (EI2)*. IEEE, 2019, pp. 643–647.

[25] M. Khorasany, Y. Mishra, and G. Ledwich, "A decentralized bilateral energy trading system for peer-to-peer electricity markets," *IEEE Transactions on Industrial Electronics*, vol. 67, no. 6, pp. 4646–4657, 2020.

[26] W. H. Kersting, *Distribution system modeling and analysis*. CRC press, 2012.

[27] J. Guerrero, A. C. Chapman, and G. Verbič, "Decentralized P2P energy trading under network constraints in a low-voltage network," *IEEE Transactions on Smart Grid*, vol. 10, no. 5, pp. 5163–5173, 2018.

[28] J. Kim and Y. Dvorkin, "A p2p-dominant distribution system architecture," *IEEE Transactions on Power Systems*, vol. 35, no. 4, pp. 2716–2725, 2020.

[29] T. Morstyn, A. Teytelboym, C. Hepburn, and M. D. McCulloch, "Integrating p2p energy trading with probabilistic distribution locational marginal pricing," *IEEE Transactions on Smart Grid*, vol. 11, no. 4, pp. 3095–3106, 2020.

[30] M. Farivar and S. H. Low, "Branch flow model: Relaxations and convexification—part I," *IEEE Transactions on Power Systems*, vol. 28, no. 3, pp. 2554–2564, 2013.

[31] X. Zhou, Z. Liu, W. Wang, C. Zhao, F. Ding, and L. Chen, "Hierarchical distributed voltage regulation in networked autonomous grids," in *American Control Conference (ACC)*. IEEE, 2019, pp. 5563–5569.

[32] H. Zhu and H. J. Liu, "Fast local voltage control under limited reactive power: Optimality and stability analysis," *IEEE Transactions on Power Systems*, vol. 31, no. 5, pp. 3794–3803, 2015.

[33] T. Baroche, P. Pinson, R. L. G. Latimier, and H. B. Ahmed, "Exogenous cost allocation in peer-to-peer electricity markets," *IEEE Transactions on Power Systems*, vol. 34, no. 4, pp. 2553–2564, 2019.

[34] K. Magzhan and H. M. Jani, "A review and evaluations of shortest path algorithms," *International journal of scientific & technology research*, vol. 2, no. 6, pp. 99–104, 2013.

[35] B. He and X. Yuan, "On the o(1/n) convergence rate of the douglas–rachford alternating direction method," *SIAM Journal on Numerical Analysis*, vol. 50, no. 2, pp. 700–709, 2012.

[36] E. Wei and A. Ozdaglar, "Distributed alternating direction method of multipliers," in *2012 IEEE 51st IEEE Conference on Decision and Control (CDC)*. IEEE, 2012, pp. 5445–5450.

[37] B. He and X. Yuan, "On non-ergodic convergence rate of douglas–rachford alternating direction method of multipliers," *Numerische Mathematik*, vol. 130, no. 3, pp. 567–577, 2015.

[38] Y. Nesterov, *Introductory lectures on convex optimization: A basic course*. Springer Science & Business Media, 2013, vol. 87.

[39] S. Mhanna, G. Verbič, and A. C. Chapman, "Adaptive admm for distributed ac optimal power flow," *IEEE Transactions on Power Systems*, vol. 34, no. 3, pp. 2025–2035, 2018.

[40] Y. Nesterov, "Smooth minimization of non-smooth functions," *Mathematical programming*, vol. 103, no. 1, pp. 127–152, 2005.

[41] T. Goldstein, B. O'Donoghue, S. Setzer, and R. Baraniuk, "Fast alternating direction optimization methods," *SIAM Journal on Imaging Sciences*, vol. 7, no. 3, pp. 1588–1623, 2014.

[42] A. J. Wood, B. F. Wollenberg, and G. B. Sheblé, *Power generation, operation, and control*. John Wiley & Sons, 2013.

[43] S. Ouali and A. Cherkaoui, "An improved backward/forward sweep power flow method based on a new network information organization for radial distribution systems," *Journal of Electrical and Computer Engineering*, vol. 2020, pp. 1–11, 2020.

[44] U. Bodkhe, S. Tanwar, K. Parekh, P. Khanpara, S. Tyagi, N. Kumar, and M. Alazab, "Blockchain for industry 4.0: a comprehensive review," *IEEE Access*, vol. 8, pp. 79 764–79 800, 2020.

Md Habib Ullah (S'15) is pursuing his Ph.D. degree in Electrical Engineering at University of Colorado Denver. He received his B.Sc. degree in Electrical and Electronics Engineering from Ahsanullah University of Science and Technology, and M.Sc. degree in Electrical Engineering from South Dakota State University in 2012 and 2016, respectively.

His research interests include transactive energy management, distributed P2P energy trading, and energy market.

Jae-Do Park (M'07, SM'14) received his Ph.D. degree in electrical engineering from the Pennsylvania State University, University Park, in 2007.

He is currently a Professor of Electrical Engineering at the University of Colorado Denver. His research interests are in the energy system applications such as renewable energy sources, energy harvesting, energy storage, and DC microgrids.

Dr. Park's research has been sponsored by NSF, ONR, and DARPA, including an NSF CAREER award in 2016.